available at www.sciencedirect.com

ScienceDirect

journal homepage: www.elsevier.com/locate/biochempharm

Fluorinated Cpd 5, a pure arylating K-vitamin derivative, inhibits human hepatoma cell growth by inhibiting Cdc25 and activating MAPK

Siddhartha Kar [a], *Meifang Wang* [a], *Seung Wook Ham* [b,1], *Brian I. Carr* [a,*]

[a] *Liver Cancer Center, Starzl Transplantation Institute, E 1552 BST, 200 Lothrop Street, University of Pittsburgh, Pittsburgh, PA, United States*
[b] *Department of Chemistry, Chung-Ang University, Seoul, South Korea*

ARTICLE INFO

Article history:
Received 21 April 2006
Accepted 26 July 2006

Keywords:
Liver cancer
Protein phosphatase
K-vitamin derivative
Cell cycle inhibition
Cdc25
MAPK

Abbreviations:
PTP, protein tyrosine phosphatase
ERK, extracellular signal related kinase
pERK, dual phosphorylated ERK
MAPK, mitogen activated protein kinase
EGF, epidermal growth factor
F-Cpd 5, fluorinated Cpd 5

ABSTRACT

We previously synthesized several K-vitamin derivatives, which are potent growth inhibitors of human tumor cells, including Hep3B human hepatoma cells. Among these, Cpd 5 was the most potent. However, being a quinone derivative, Cpd 5 has the potential for generating toxic reactive oxygen species (ROS). We therefore synthesized a fluorinated derivative of Cpd 5, F-Cpd 5. The calculated reduction potential of F-Cpd 5 was much higher than that for Cpd 5 and it was not predicted to generate ROS. This was supported by our observation that F-Cpd 5 generated significantly lower ROS than Cpd 5. F-Cpd 5 was three times more potent than Cpd 5 in inhibiting Hep3B cell growth. Interestingly, under identical culture conditions, F-Cpd 5 inhibited mitogen-induced DNA synthesis in normal rat hepatocytes 12-fold less potently than Hep3B cells. F-Cpd 5 was found to induce caspase-3 cleavage and nuclear DNA laddering, evidences for apoptosis. It preferentially inhibited the activities of the cell cycle controlling phosphatases Cdc25A and Cdc25B, by binding to their catalytic cysteines. Consequently, inhibitory tyrosine phosphorylation of the Cdc25 substrate kinases Cdk2 and Cdk4 were induced. F-Cpd 5 also induced phosphorylation of the MAPK proteins ERK1/2, JNK1/2 and p38 in Hep3B cells and the MAPK inhibitors (U0126, JNKI-II, and SB 203580) antagonized its growth inhibition. F-Cpd 5 inhibited the action of cytosolic ERK phosphatase activity, which likely caused the ERK phosphorylation. F-Cpd 5 thus differentially inhibited growth of normal and tumor cells by preferentially inhibiting the actions of Cdc25A and Cdc25B phosphatases and inducing MAPK phosphorylation.

1. Introduction

One of the mechanisms of intracellular control of protein function and signaling is protein phosphorylation and dephosphorylation catalyzed by protein kinases and phosphatases, respectively [1]. Two classes of mammalian protein phosphatases have been identified, which are serine/threonine (PS/TP) and tyrosine specific (PTP). There is also a subclass of PTP (DSP or dual specific protein phosphatase), which dephosphorylates both tyrosine and serine/threonine residues on the same protein [2]. DSPs and PTPs have similar mechanisms of action and share similar active site sequence motifs, although there

* *Corresponding author*. Tel.: +1 412 624 6684; fax: +1 412 624 6666.
E-mail address: carrbi@upmc.edu (B.I. Carr).
[1] On sabbatical leave to University of Pittsburgh.
0006-2952/$ – see front matter © 2006 Elsevier Inc. All rights reserved.
doi:10.1016/j.bcp.2006.07.024

is no sequence identity beyond the active site region [3]. DSPs appear to have a marked preference for cyclin-dependent kinases and MAP-kinases, which regulate cell cycle and mitogenic signal transduction [4–6].

The cyclin-dependent kinases (Cdk) have important functions in the progression of the eukaryotic cell cycle [7]. One of the major mechanisms of cell cycle progression is the regulation of the activities of Cdk1, Cdk2, and Cdk4 by phosphorylation and dephosphorylation. The Cdc25 phosphatases dephosphorylate these Cdks and thereby activate them. Mammalian cells express three Cdc25 proteins, Cdc25A, Cdc25B and Cdc25C. Cdc25A mainly controls the G1/S progression, whereas Cdc25B and Cd25C activate the G2/M transition [8,9]. Mutation analysis has recently revealed that Cdc25A by itself can control both the G1/S and G2/M phases and is sufficient for executing a normal cell cycle [10–12].

Cdc25A and Cdc25B can also behave as oncogene [13]. Elevated Cdc25A and Cdc25B mRNA and protein have been found in many human tumor types [14–16], which makes them attractive targets for anticancer therapies.

Several quinoid compounds, including Cpd 5 [2-(2-mercaptoethanol)-3-methyl-1,4-naphthoquinone], a growth inhibiting K-vitamin analog, have been shown to be effective Cdc25 inhibitors [17–21]. One of these compounds (Cpd 5) has been reported to inhibit Cdc25 actions by sulfhydryl arylation of the catalytic cysteine [22]. Cpd 5 has been shown to inhibit hepatoma cell growth both in vitro and in vivo [23]. However, the redox properties of the quinones can also potentially generate toxic oxygen species [24,25]. Redox cycling and oxidative stress are initiated by the single electron reduction of quinones by NADH-cytochrome P450 oxidoreductase, NADH-cytochrome b5 oxidoreductase, and NADH-ubitiquinone oxidoreductase [26]. This may cause toxicity to normal tissue and thus reduce their therapeutic use. We have therefore synthesized a fluorinated Cpd 5 derivative (F-Cpd 5), the reduction potential of which was expected to be much greater than of Cpd 5, due to the inductive effects of the electronegative fluorine atoms, preventing superoxide generation [27].

We found that F-Cpd 5 inhibited Hep3B hepatoma cell growth in vitro with a three-fold higher potency than Cpd 5 and it was predicted, using the semi-empirical AM1 method, to be a pure arylator of cysteine-containing proteins, without generating reactive oxygen species [27]. We examine the cellular growth inhibitory mechanisms of Hep3B cells by F-Cpd 5, and found that it induced apoptosis, preferentially inhibited Cdc25 family of phosphatases and induced MAPK phosphorylation.

2. Materials and methods

2.1. Synthesis of F-Cpd 5 [5,6,7,8-tetrafluoro-2-(2-hydroxy-ethylsulfanyl)-3-methyl-(1,4)naphthoquinone]

F-Cpd 5 was synthesized as previously described [27]. Briefly a solution of 2,5,6,7,8-pentafluoro-3-methyl-(1,4)naphthoquinone (Chemical Diversity, San Diego, CA) in methanol was treated with 1.2 equivalent of β-mercaptoethanol. The reaction mixture was stirred under an atmospheric pressure of argon for 30 min at room temperature. After evaporation of solvent, the resulting crude product was chromatographed on the silica gel with hexane:ethyl acetate (9:1) to give F-Cpd 5 in 80–90% isolation yields. Purity of the final product was analyzed by mass-spectroscopy.

2.2. Cell culture and growth inhibition assays

Hep3B, PLC/PRF5, SKBR3, FemX, HR, and LS140 cells were cultured in Minimum Essential Medium (MEM) (Invitrogen, Carlsbad, CA) in a humidified atmosphere of 5% CO_2 and 95% air at 37 °C. The medium contained 10% fetal bovine serum (Invitrogen, Carlsbad, CA). Cells were plated at 2×10^4 cells/well in 24-well dishes (Corning Inc., Science Products Div., Corning, NY) for cell growth inhibition assays. After cell attachment, the medium was replaced with growth medium (MEM + 10% FBS) with or without test compounds. Cells were also treated for 1 h with the MAPK inhibitors U0126, JNKI-I or SB 203580 (Calbiochem, La Jolla, CA) before addition of F-Cpd 5. After 3 days of culture, the medium was removed and the cells were immediately washed with ice-cold phosphate-buffered saline (PBS) to terminate growth. Cells were then harvested and stored at −80 °C until used. Cell number was measured by a DNA fluorometric assay with Hoechst 33258, as previously described [28].

2.3. Hepatocyte preparation and DNA synthesis

Hepatocytes from the livers of 2–3-month-old male Fischer F344 rats (weight 180–220 g) were isolated by a two-step in situ collagenase perfusion technique [29]. Briefly, under isoflurane anesthesia, the rat liver was cannulated via the portal vein. The liver was perfused first with 150 ml of Hanks buffer (Invitrogen, Carlsbad, CA) containing 20 mg/ml of EGTA for 3 min, then perfused with 300 ml of collagenase B solution (40 mg/100 ml; Roche Applied Science, Indianapolis, IN) for 6 min (50 ml/min). Hepatocytes were dispersed and washed three times with L15 medium (Invitrogen, Carlsbad, CA), and resuspended in serum-free William's E medium (Invitrogen, Carlsbad, CA). Cell number was determined with a hemocytometer and viability was determined by the trypan blue exclusion method. Hepatocytes were plated at a density of 2.5×10^5 cells per 35 mm diameter fibronectin-coated tissue-culture dish. They were cultured at 37 °C in a 5% (v/v) CO_2 atmosphere. After a 3-h serum-free attachment period, the medium was changed to 1 ml of fresh William's E medium. EGF (Roche Applied Science, Indianapolis, IN), with or without F-Cpd 5 was added to the culture medium. To determine in vitro DNA synthesis, 5 μCi of ^{3}H-thymidine (MP Biomedicals, Solon, OH) was added to each plate and maintained there for a 24 h culture period from 48 to 72 h. After 72 h of culture, hepatocytes were harvested, and ^{3}H-thymidine incorporation in DNA was measured using a liquid scintillation counter. Total hepatocyte protein amounts were determined by the Bradford method [30].

2.4. Cell lysate preparation, Western blots and immunoprecipitation

Western blot and immunoprecipitation protocols were followed as described previously [17,31]. Cells were plated at a

density of 5×10^4 cells/well in six-well tissue culture plates. After 24 h, the culture medium was replaced with fresh medium, without or with F-Cpd 5 at various concentrations and incubated for different times. Cells were then rinsed with phosphate-buffered saline and lysed in 100 μl of RIPA buffer (150 mM NaCl, 50 mM Tris–HCl pH 8.0, 0.1% SDS, 1% Triton X-100, 1 mM orthovanadate, 1 mM phenylmethylsulfonyl fluoride, 10 μg/ml leupeptin, 10 μg/ml aprotinin). The lysates were cleared by centrifugation at 12,000 rpm for 5 min in a microcentrifuge. Protein concentration of the lysates was determined by the Bradford assay [30].

Lysate proteins (40 μg/lane) were separated on a 10% gel by SDS-polyacrylamide gel electrophoresis. The proteins were Western blotted onto a polyvinylidene difluoride membrane (Amersham, Piscataway, NJ). The membrane was then incubated for 1 h at room temperature in TBST buffer (10 mM Tris–HCl, PH 8.0, 150 mM NaCl, 0.05% Tween 20), containing 1% bovine serum albumin (Fraction V, Sigma, St. Louis, MO). The same membrane was subsequently incubated for 1 h with specific antibody, which was diluted in the same buffer. It was then washed four times with TBST (without BSA) and then incubated for another 1 h with horseradish peroxidase-conjugated secondary antibody (Amersham, Piscataway, NJ) which was diluted in TBST–BSA. The membrane was again washed four times with TBST. Enhanced chemiluminescence reagent (Perkin-Elmer, Boston, MA) was used for detection.

For immunoprecipitation, 200 μg of cell lysate proteins was incubated with antibody and protein A–agarose (Sigma, St. Louis, MO) overnight at 4 °C. The immunoprecipitate then was washed three times with RIPA buffer.

The antibodies used in these experiments (ERK2, JNK1, p38, MKP1, Cdc25A, Cdc25B) were purchased from Santa Cruz Biotechnology, Santa Cruz, CA, and all phospho-antibodies were from Cell Signaling, Beverly, MA.

2.5. PTP activity assay

The activity of protein phosphatases was measured by using the substrate 3-*O*-methyl fluorescein phosphate (OMFP) (Molecular Probes, Eugene, Oregon), as previously described [32]. The Cdc25 proteins were a gift from Dr. J. Rudoph (Duke University, North Carolina) and PTP1B and MKP1 phosphatases were obtained commercially (Upstate, Lake Placid, NY). The F-Cpd 5 analog was solubilized in DMSO, and all reactions including controls were performed in 1% DMSO. The final incubation mixture (150 μl) was optimized for enzyme activity and comprised of 30 mM Tris (pH 8.5), 75 mM NaCl, 1 mM EDTA, 0.33% BSA and 1 mM DTT. Reactions were initiated by addition of enzyme. Fluorescence emission from the product was measured over a 10–60 min time period at room temperature in a multi-well plate reader. The reaction was linear over the time period of the experiment and was directly proportional to both enzyme and substrate concentration. Half-maximal inhibition constants were calculated by curve fit by Cricket Graph III program.

2.6. Phospho-Cdk4 dephosphorylation assay

Tyrosine-phosphorylated phospho-Cdk4 was prepared from Hep3B cells, which were arrested in the G1 phase of cell cycle, by treating the cells with 2 mM hydroxyurea for 18 h. Phospho-Cdk4 protein was immunoprecipitated with anti-Cdk4 antibody and protein A–sepharose. The immunoprecipitated phospho-Cdk4 protein was incubated for 1 h at 37 °C with Hep3B cell lysate proteins, either in presence or in absence of F-Cpd 5. After the phosphatase reaction, the protein A–sepharose bound phospho-Cdk4 protein was precipitated again and then run oh a Western blot, which was probed with anti-phospho-tyrosine antibody.

2.7. Phospho-ERK dephosphorylation assay

Phospho-ERK2 was obtained New England Biolabs (Ipswich, MA). Hep3B cell lysate was immunoprecipitated with anti-ERK2 antibodies and cleared of endogenous ERK2 proteins by centrifugation, as previously described [33]. Phospho-ERK2 was incubated with ERK2-cleared cell lysate proteins or the ERK2 phosphatase MKP1, in phosphatase buffer (50 mM Tris–HCl, pH 7.5, 1 mM EDTA, 10 mM dithiothreitol) for 30 min at 37 °C in the presence or absence of F-Cpd 5. The phosphatase reaction was terminated by the addition of an equal volume of 2× sample buffer. The proteins were separated by 10% SDS-PAGE and transferred to a Western blot that was probed with phospho-ERK1/2 and ERK2 antibodies.

2.8. Competition of Cpd 5-Bt and F-Cpd 5 binding to Cdc25A or Cdc25B

Cdc25A or Cdc25B (180 ng) was incubated in a 10 μl reaction volume for 18 h at 4 °C, with 1 μM Cpd 5-Bt (a biotin-tagged Cpd 5 derivative) and F-Cpd 5 at a concentration of 0, 1, 10 and 100 μM or MKP1 protein (10 μM). Cpd 5-Bt bound to Cdc25A was immuoprecipitated with anti-biotin antibody (Sigma, St. Louis, MO) and the immunoprecipitated proteins were probed on Western blots with anti-Cdc25A or anti-Cdc25B antibodies.

2.9. Hep3B cell apoptosis assay

Hep3B cells were treated with either Cpd 5 or F-Cpd 5 and genomic DNA was extracted by standard procedure [34]. DNA was electrophoresed on a 1% agarose gel and stained with ethidium bromide. Cell lysate proteins were also extracted from the treated cells and were analyzed on a Western blot, which was probed with anti-caspase-3 antibody.

2.10. Measurement of cellular ROS generation

Hep3B cells were either untreated or treated for 2 h with equivalent concentrations (2× IC_{50}) of Cpd 5 (12 μM) and F-Cpd 5 (4 μM). The Image-it ROS detection kit from Molecular Probes Inc. (Eugene, OR) was used to label cells with 5-(and-6)-carboxy-2′,7′-dichlorodihydrofluorescein diacetate, a reliable fluorogenic marker for ROS in live cells. Fluorescence was measured by a fluoresent spectrophotometer.

A cell-permeable superoxide mimetic MnTBPAC (manganese(III) tetrakis (4-benzoic acid) porphyrin chloride) (Axxora, San Diego, CA), was added at concentrations of 1 or 10 μM to inhibit superoxide production induced by Cpd 5 and F-Cpd 5. ROS generation and cell numbers were measured.

2.11. Statistical analysis

Data were analyzed statistically by "t-test" and significance was determined by calculating the "p" value by Microsoft Excel program.

3. Results

3.1. F-Cpd 5 synthesis

F-Cpd 5 was synthesized from β-mercaptoethanol and pentafluoronaphthoquinone as described before [27] and briefly in the methods section (Fig. 1A).

3.2. Growth inhibition of various tumor cell lines by F-Cpd 5

F-Cpd 5 was shown previously to inhibit the growth of the hepatoma cell line Hep3B with IC_{50} of 2 μM, which was three-fold lower than that of Cpd 5 [27]. We tested F-Cpd 5 effects on growth of several other human tumor cell lines. Tumor cell lines from mammary carcinoma (SKBR3), hepatocellular carcinoma (PLC/PRF5 and Hep3B), melanoma (FemX), gastric carcinoma (HR), and colon cacinoma (LS140) were plated in tissue culture dishes. Increasing concentrations of F-Cpd 5, ranging from 0.5 to 10 μM (dissolved in DMSO) were added to the dishes. After 3 days of incubation, the number of cells that remained on the dish was counted. An inhibition curve was plotted for each cell line and the IC_{50} values were calculated, which ranged from 1 to 15 μM (Fig. 1B). F-Cpd 5 was more potent in inhibiting liver and skin tumor cell lines compared to breast, stomach, and colon cancer cell lines.

3.3. Hep3B cells and normal hepatocytes are differentially sensitive to growth inhibition

An anticancer compound will have potential clinical use if it has relatively low cytotoxicity against normal cells. Therefore,

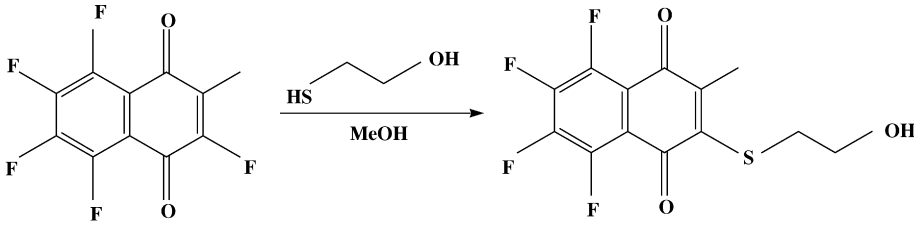

(A) **Pentafluoronaphthoquinone** **Fluorinated-Cpd 5 or F-Cpd 5**

(B)

Tumor	Cell line	IC_{50}(μM)
Hepatocellular carcinoma	Hep3B	2
Hepatocellular carcinoma	PLC/PRL5	1
Melanoma	FemX	1
Colon carcinoma	LS140	10
Mammary carcinoma	SKBR3	15
Gastric carcinoma	HR	15

(C)

Tyrosine/dual specificity phosphatase	IC_{50} (μM) F-Cpd 5	Cpd 5
Cdc25A	0.8	5
Cdc25B	1	2
Cdc25C	50	2
MKP1	>100	>100
PTP1B	>100	>100

Fig. 1 – Structure and inhibitory activity of F-Cpd 5 against tumor cells and various PTP/DSP. (A) F-Cpd 5 was derived from pentafluoronaphthoquinone. (B) Growth inhibitory IC_{50} was determined for cell lines from hepatoma (Hep3B, PLC/PRF5), melanoma (FemX), mammary carcinoma (SKBR3), gastric carcinoma (HR) and colon carcinoma (LS140). (C) Inhibitory IC_{50} of enzyme activity was also determined for F-Cpd 5 and compared with Cpd 5 for the various PTP/DSP, Cdc25A, Cdc25B, Cdc25C, MKP1, and PTP1B.

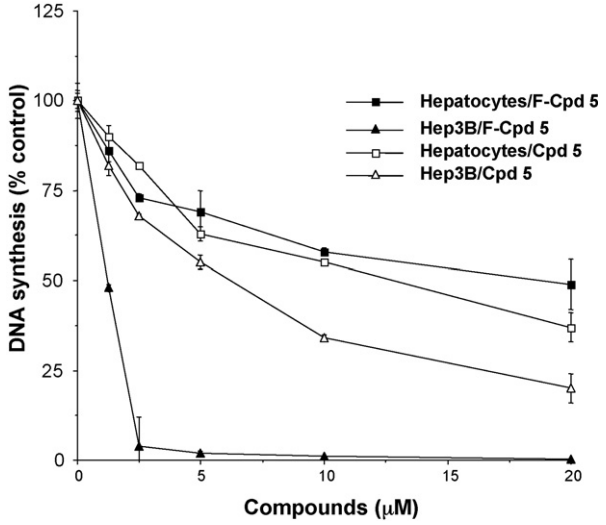

Fig. 2 – Differential sensitivity of normal liver cells and liver tumor cells. Normal hepatocytes were isolated from rat, plated on fibronectin matrix, and cultured in serum-free medium in the presence of EGF. Hep3B hepatoma cells were also cultured under the same conditions. Increasing concentrations of either Cpd 5 or F-Cpd 5 was added to the hepatocyte and hepatoma cultures and DNA synthesis was determined by incorporation of ^{3}H-thymidine for a 24 h period after 2 days of culture.

the inhibitory effects of F-Cpd 5 on DNA synthesis of mitogen stimulated normal rat hepatocytes in primary culture were determined. Rat hepatocytes were isolated and plated in culture. Three hours after plating, EGF was added to stimulate DNA synthesis, which was measured by the incorporation of ^{3}H-thymidine 48 h after addition of EGF, in the presence or absence of Cpd 5 or F-Cpd 5. The IC_{50} of F-Cpd 5 was found to be about 15 μM for normal hepatocytes compared to 1.25 μM for Hep3B cells under identical culture condition. Normal hepatocytes were thus about 12-fold more resistant to the growth inhibitory actions of F-Cpd 5 than Hep3B hepatoma cells. On comparison, under similar culture conditions, Cpd 5 inhibited Hep3B DNA synthesis with an IC_{50} of 5 μM, which was four-fold less potent than F-Cpd 5 (Fig. 2).

3.4. *Inactivation of Cdc25 phosphatases in vitro and in Hep3B cells*

We previously found that Cpd 5 preferentially inhibited the activities of the Cdc25 phosphatases [32]. The structure of the F-Cpd 5 suggested that it is also likely to be a Cdc25 inhibitor. We therefore compared the inhibitory activity of F-Cpd 5 against the dual specificity phosphatases Cdc25A, Cdc25B, Cdc25C, MKP1 and the protein tyrosine phosphatase PTP1B. The IC_{50} of F-Cpd 5 was found to be 0.8, 1, and 50 μM for Cdc25A, Cdc25B, and Cdc25C, respectively. However, the IC_{50} was more than 100 μM for MKP1 and PTP1B (Fig. 1C). Thus F-Cpd 5 was found to preferentially inhibit the Cdc25A and Cdc25B phosphatases. On comparison, Cpd 5 inhibited Cdc25A activity with an IC_{50} of 5 μM, which was six-fold more than F-Cpd 5 (IC_{50} = 0.8 μM) (Fig. 1C). However, Cpd 5 inhibited Cdc25B (IC_{50} = 2 μM) activity with similar potency as F-Cpd 5 (IC_{50} = 1 μM), but inhibited Cdc25C (IC_{50} = 2 μM) activity 25-fold more potently than F-Cpd 5 (IC_{50} = 50 μM). Like F-Cpd 5, Cpd 5 did not inhibit (>100 μM) the activities of MKP1 or PTP1B (Fig. 1C).

We also examined whether F-Cpd 5 could inhibit the Cdc25 phosphatases in Hep3B cells. Cdc25A and Cdc25B inactivation result in induction of tyrosine phosphorylation of the Cdc25 substrate Cdk2 and Cdk4 [10]. Hep3B cells were treated in culture with F-Cpd 5 and tyrosine phosphorylation of the Cdc25A and Cdc25B substrates Cdk2 and Cdk4 was determined after immunoprecipitation with either Cdk2 or Cdk4 antibody and subsequent probing with phospho-tyrosine antibody. Both Cdk2 and Cdk4 were found to be tyrosine phosphorylated as a result of F-Cpd 5 action (Fig. 3A) suggesting that F-Cpd 5 likely inhibited Cdc25A and Cdc25B activities in Hep3B cells.

Inhibition of Cdc25 phosphatases in Hep3B cell lysates was also measured directly. Immunoprecipitated tyrosine-phosphorylated Cdk4 was prepared from cells, which were growth arrested in the G1 phase of the cell cycle by hydroxyurea. This phospho-Cdk4 protein was then used in a dephosphorylation assay with Hep3B cell lysate proteins, which was either treated

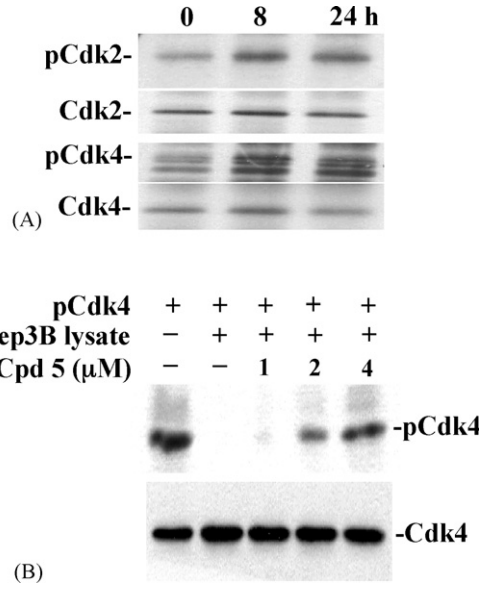

Fig. 3 – F-Cpd 5-induced tyrosine phosphorylation of Cdk2 and Cdk4 and inhibited Cdc25 activity. (A) Hep3B cells were treated with 2 μM of F-Cpd 5 for 8 or 24 h. Treated or untreated lysates were immunoprecipitated using, either Cdk2 or Cdk4 antibodies. The immunoprecipitates were run on Western blots, which was probed with anti-phospho-tyrosine antibody. Unphosphorylated Cdk2 and Cdk4 were probed as controls. (B) Tyrosine-phosphorylated Cdk4 was purified by immunoprecipitation from cell lysates from Hep3B cells, which were treated with 2 mM hydroxyurea for 18 h. The phosho-Cdk4 protein was used in a dephosphorylation reaction with Hep3B cell lysate proteins containing Cdc25, which was either treated or untreated with F-Cpd 5. The remaining phospho-Cdk4 protein from this phosphatase reaction was assayed on a Western blot with anti-phospho-tyrosine antibody. Cdk4 was also probed as a control.

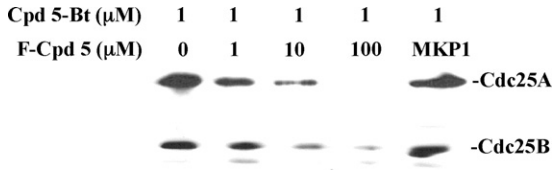

Fig. 4 – Competition between F-Cpd 5 and Cpd 5-Bt for binding to Cdc2A or Cdc25B. Cpd 5-Bt (1 μM) was incubated at 4 °C for 18 h, with 180 ng of either Cdc25A or Cdc25B, in the presence of 10 μM MKP1 or increasing concentrations (0, 1, 10 and 100 μM) of F-Cpd 5. Enzyme bound Cpd 5-Bt was immunoprecipitated with anti-biotin antibody. The immunoprecipitated proteins were run on Western blots, and the blots were probed with either Cdc25A or Cdc25B antibody.

or untreated with F-Cpd 5. Hep3B cell lysate proteins was found to contain phosphatase, which is likely to be Cdc25, specific for the tyrosine-phosphorylated Cdk4 and this activity was inhibited by F-Cpd 5 (Fig. 3B).

3.5. *F-Cpd 5 binds to the catalytic cysteine of Cdc25A*

We previously found that PD 49, a biotin-tagged derivative of Cpd 5, bound to the catalytic cysteine of Cdc25B [22]. PD 49 had the thioethanol side-chain of Cpd 5 substituted by Br. For this study, we have synthesized a biotin-tagged Cpd 5 derivative (Cpd 5-Bt), which now had the thioethanol side-chain. We assume that Cpd 5-Bt will have identical binding to the catalytic cysteine as PD 49. We explored whether both Cpd 5-Bt and F-Cpd 5 might bind to the catalytic cysteine in Cdc25A or Cdc25B. Cpd 5-Bt was incubated with Cdc25A or Cdc25B in the presence of increasing concentrations of F-Cpd 5. The Cpd 5-Bt–Cdc25 complex was immunoprecipitated with anti-biotin antibody and Cdc25 protein in the immunoprecipitate was visualized on Western blots, using anti-Cdc25 antibody. Increasing concentrations of F-Cpd 5 were found to decrease the binding of Cpd 5-Bt to both Cdc25A and Cdc25B (Fig. 4). This would suggest a competitive binding by F-Cpd 5 to the catalytic cysteine of either Cdc25A or Cdc25B. MKP1, another dual specificity phosphatase, even at 10 μM, did not compete with Cpd 5-Bt for binding to Cdc25A or Cdc25B (Fig. 4).

3.6. *Induction of apoptosis and ROS production*

We investigated whether cell growth inhibition of the hepatoma cells Hep3B and PLC/PRL5 by F-Cpd 5 was associated with induction of apoptosis. Caspase-3 cleavage and nuclear DNA laddering are two hallmark assays of apoptosis. We treated the cells with F-Cpd 5 and assayed for caspase-3 cleavage and nuclear DNA laddering and found evidence for both in the F-Cpd 5-treated compared to the untreated cells (Fig. 5A and B).

F-Cpd 5 was designed from theoretical considerations to have a lesser likelihood for ROS generation than its parent Cpd 5. Therefore, we measured ROS generation in Hep3B and PLC/

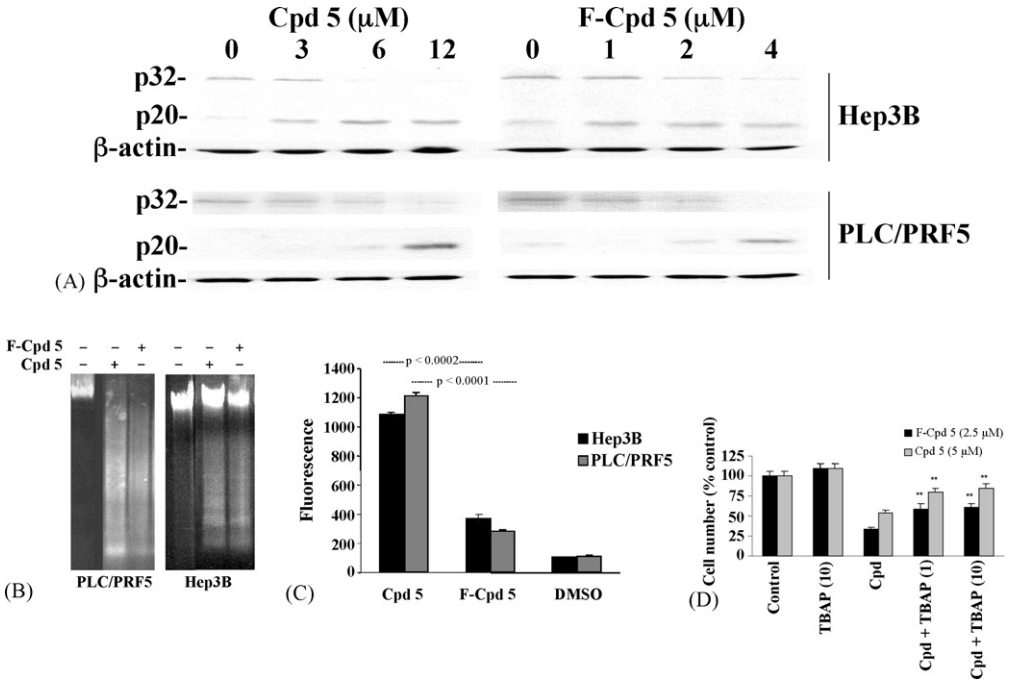

Fig. 5 – Induction of hepatoma cell apoptosis and ROS production. Hep3B and PLC/PRF5 hepatoma cells were either untreated or treated with F-Cpd 5 or Cpd 5 and both the cell lysate proteins and the nuclear DNA were extracted. (A) Proteins were resolved on Western blots, which were probed with anti-caspase-3 and β-actin (control) antibodies. (B) Nuclear DNAs were resolved on a 1% agarose gel and stained with ethidium bromide. (C) ROS generated was measured by the ROS-sensitive fluorogenic dye carboxy-H_2DCFDA. (D) Cell-permeable superoxide dismutase inhibitor MnTBPAC (1 or 10 μM) was added together with the compounds in cell culture and ROS generation and cell number were measured. Only cell numbers were shown in this figure. Statistical significance, $^{**}p < 0.01$ was calculated by "t-test".

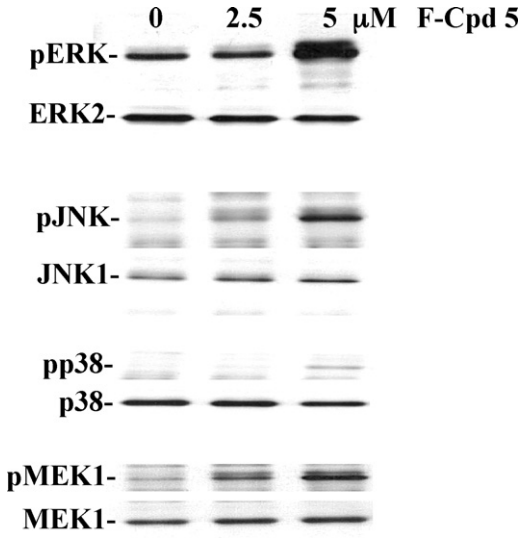

Fig. 6 – Induction of MAPK phosphorylation. Hep3B cells were treated with 2.5 and 5 μM of F-Cpd 5 for 1 h. Western blots of the cell lysate proteins were probed with pMEK1, pERK1/2, pJNK and pp38 antibodies. The unphosphorylated MEK1, ERK2, JNK1 and p38 proteins were probed in the same blots for control.

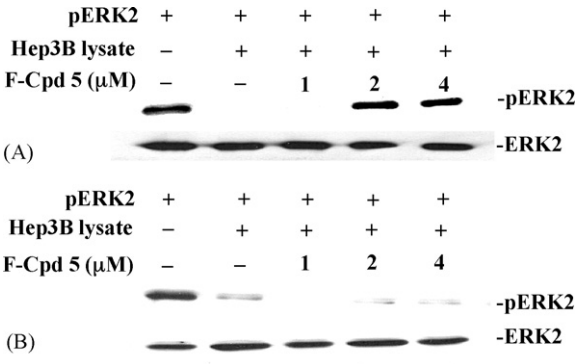

Fig. 7 – F-Cpd 5 inhibited ERK2 phosphatase activity of Hep3B lysates. The endogenous ERK2 protein was cleared from Hp3B lysate proteins by immunoprecipitation with anti-ERK2 antibody. The ERK2-cleared lysate proteins were mixed with exogenous pERK2 protein, either in presence of absence of F-Cpd 5 in a phosphatase assay (A). Another ERK2 phosphotase protein, MKP1 was also used in the ERK2 dephosphorylation assay. MKP1 protein was incubated with exogenous pERK2 protein either in presence or absence of F-Cpd 5 (B). The phosphorylation status of ERK2 in both experiments was determined by Western blots, which were probed with pERK2 and ERK2 (control) antibodies.

PRL5 cells, which were either untreated or treated with Cpd 5 or F-Cpd 5. ROS generated by F-Cpd 5 was found to be significantly less than with Cpd 5 treatment in both cell lines (Fig. 5C). ROS generation and growth inhibition induced by Cpd 5 and F-Cpd 5 could be partially antagonized by MnTBPAC (manganese(III) tetrakis (4-benzoic acid) porphyrin chloride), a cell-permeable superoxide dismutase mimetic (Fig. 5D).

3.7. *Induction of phospho-ERK1/2 and ERK1/2 pathway*

We previously found that the Cdc25 phosphatase inhibitor Cpd 5 induced phosphorylation and activation of ERK1/2, and subsequently showed that Cdc25A, which could act as a phosphatase for pERK [35], was inhibited by Cpd 5 action. Therefore, Western blots of Hep3B cell lysate proteins from F-Cpd 5-treated cells were probed with phospho-ERK1/2 (pERK1/2) antibody. pERK1/2 was found to be strongly induced in the F-Cpd 5-treated, compared to untreated cells (Fig. 6). There was no effect on the amount of ERK2 protein. Moreover, two other MAP-kinases, JNK1/2 and to a small extent p38, as well as MEK1 (the upstream kinase of ERK) were also phosphorylated (Fig. 6) when Western blots were probed with antibodies to either phospho-JNK1/2 or phospho-p38 or phospho-MEK1. Amounts of non-phosphorylated JNK1, p38 or MEK1 did not change on F-Cpd 5 treatment (Fig. 6).

3.8. *Inhibition of ERK1/2 phosphatase(s) activity in Hep3B cell lysates*

The strong induction of ERK1/2 phosphorylation by F-Cpd 5 could be due either to induction of its upstream kinase MEK1/2 or to inhibition of its phosphatase(s), or both. We found that the ERK1/2 kinase MEK1/2 was activated by F-Cpd 5 (Fig. 6). In order to determine whether endogenous cellular ERK1/2 phosphatase(s) might also be inhibited, Hep3B cell lysates were cleared of endogenous ERK2 protein by immunoprecipitation with ERK2 antibody. The cleared lysate proteins (containing cellular phosphatases) were incubated with commercially obtained exogenous pERK2 as target, in the presence or absence of F-Cpd 5. The phosphorylation status of ERK2 was determined on a Western blot after it was probed with pERK2 or ERK2 antibodies. Hep3B cell lysates were found to dephosphorylate exogenous pERK2 and this phosphatase activity was inhibited by F-Cpd 5 action (Fig. 7A). In contrast, the ERK2 phosphatase activity of the MAP-kinase phosphatase MKP1 was not inhibited by F-Cpd 5 at similar concentrations (Fig. 7B). This suggested the presence of ERK2 phosphatase(s) other than MKP1 in Hep3B cell lysate proteins, which were inhibited by F-Cpd 5 action, leading to ERK phosphorylation.

3.9. *Expression of endogenous MKP1 and Cdc25A proteins and induction of pERK by F-Cpd 5 in tumor cell lines*

The results in the previous section (Fig. 7B) suggested that Hep3B cells contained ERK2 phosphatases other than MKP1. We therefore determined the endogenous expression of MKP1 and Cdc25A in the F-Cpd 5-sensitive and F-Cpd 5-resistant tumor cells. MKP1 was found to be expressed in the relatively resistant cells (SKBR3, LS140 and HR) compared to the sensitive cells (Hep3B, PLC/PRL5 and FemX) (Fig. 8). We have previously found that Cdc25A might be a candidate phosphatase for ERK [35]. Therefore, we also examined the endogenous levels of Cdc25A in the tumor cell lines and found that Cdc25A was expressed in the F-Cpd 5-sensitive cells (Hep3B, PLC/PRL5, and FemX), but not in the resistant cells (SKBR3, LS140 and HR) (Fig. 8).

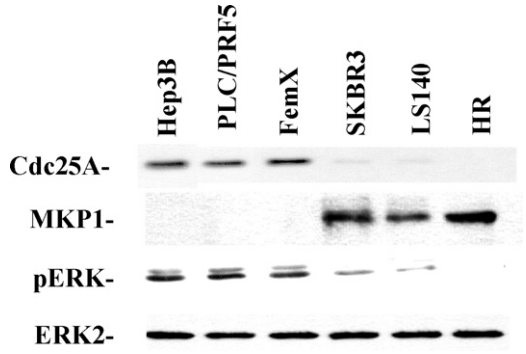

Fig. 8 – MKP1, Cdc25A and ERK2 protein expression and induction of pERK by F-Cpd 5 in tumor cell lines. Endogenous levels of MKP1, Cdc25A and ERK2 was measured by Western blots in Hep3B, PLC/PRF5, FemX, SKBR3, LS140 and HR cell lines. pERK induction was also determined in these cells after treatment with 2 μM of F-Cpd 5 for 1 h.

3.10. *MAPK phosphorylation was involved in the growth inhibitory mechanisms*

We examined whether MAPK phosphorylation that was induced by F-Cpd 5 action might be involved in its mechanism of growth inhibition. The F-Cpd 5-sensitive and -resistant cell lines were treated with F-Cpd 5 for 1 h and the levels of pERK induced were determined by Western blots. pERK was found to be induced in the sensitive (Hep3B, PLC/PRL5, and FemX) but not in the resistant (SKBR3, LS140 and HR) cells (Fig. 8), suggesting an association between pERK induction and sensitivity to growth inhibition. Hep3B cells were also pre-treated with the MEK1/2 inhibitor U0169, in order to antagonize ERK1/2 phosphorylation induced by F-Cpd 5. We found that growth inhibition induced by F-Cpd 5 was antagonized ($p < 0.001$) by pre-treatment of the cells with this MEK inhibitor (Fig. 9). This suggested that ERK1/2 phosphorylation probably was involved in the growth inhibition mediated by F-Cpd 5. In contrast to Cpd 5, F-Cpd 5 was also found to induce phosphorylation of two other MAPKs, JNK and p38. Hep3B cells were therefore also pre-treated with the JNK and p38 inhibitors, JNKI-I and SB 203580 before F-Cpd 5 treatment. These MAPK inhibitors were also found to antagonize ($p < 0.001$) the growth inhibition induced by F-Cpd 5 (Fig. 9). Therefore, induction of all three MAPKs, ERK, JNK and p38, probably contribute to F-Cpd 5-induced growth inhibition.

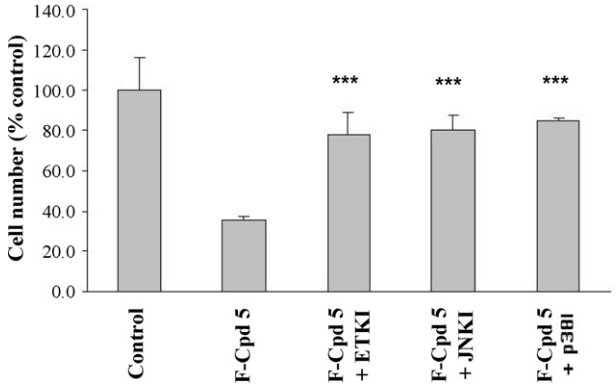

Fig. 9 – MAPK inhibitors antagonize F-Cpd 5-induced growth inhibition. Hep3B cells were treated with 2 μM of F-Cpd 5, either without or with pre-treatment with the MAPK inhibitors U0126 (ERKI), JNKI-II (JNKI) or SB 203580 (p38 inhibitor). Cell growths were determined after 3 days. Statistical significance was calculated by Student's *t*-test, $^{***}p < 0.001$.

4. Discussion

We have previously synthesized several K-vitamin analogs, which were growth inhibitors both in vitro and in vivo [17–22]. The prototype of these inhibitors, Cpd 5 was found to inhibit phospho-ERK phosphatase activity and Cdc25 phosphatases by binding to the catalytic cysteine of the Cdc25 enzyme [22]. The thiol-antioxidants glutathione or *N*-acetyl-L-cysteine, but not the non-thiol-antioxidants catalase or superoxide dismutase, antagonized Cpd 5-mediated growth inhibition of Hep3B cells [17]. These results were considered to indicate that Cpd 5 inhibited sulfhydryl-containing cellular enzymes by arylation of cysteines and not by generation of reactive oxygen species. As pointed out by Ham et al. [27], catalase and superoxide dismutase cannot easily penetrate into cells. Thus involvement of ROS in Cpd 5-induced cytotoxicity remains an open question.

Therefore, we synthesized a new Cpd 5 derivative, F-Cpd 5, which would theoretically be incapable of generating reactive oxygen species. The structural features of Cpd 5 were preserved in F-Cpd 5. The quinone ring of Cpd 5 seemed necessary for reaction with the active site cysteine of Cdc25 [21]. The active Cdc25 inhibitors also appeared to be flat molecules, perhaps to fit into the catalytic site of the enzyme. The thioethanol side chain also seemed to be important. Substitution at this site with other side groups was found to greatly reduce reactivity [21]. If we preserved all these features in the molecule, the one-electron reduction potential was calculated to be 260 mV lower than that of 1,4-benzoquinone (a pure arylator). Therefore, Ham et al. [27] synthesized a Cpd 5 derivative with four fluorine atoms on the benzene ring of Cpd 5 (Fig. 1A). The one-electron reduction potential of this new compound (F-Cpd 5) was calculated to be ~600 mV greater that that of Cpd 5, due to the inductive effects of the electronegative fluorine atoms. The reduction potential of F-Cpd 5 was in fact more than 337 mV higher than that of 1,4-benzoquinone. Hence F-Cpd 5 was predicted to be a pure arylator that would not generate reactive oxygen species. Indeed, when we measured ROS generation in Hep3B by F-Cpd 5, it was found that F-Cpd 5 generated significantly less ROS as compared to Cpd 5 (Fig. 5C). This ROS generation and growth inhibition could be antagonized with a cell-permeable superoxide dismutase mimetic, MnTBPAC [manganese(III) tetrakis (4-benzoic acid) porphyrin chloride] (Fig. 5D). This suggests a role of ROS generated by Cpd 5 in growth inhibition. Since F-Cpd 5 generated much less ROS, this secondary mechanism of cell killing is much less important than Cpd 5. The higher inhibitory potency of F-Cpd 5 is therefore due to mechanisms other that ROS production.

F-Cpd 5 was found to preferentially inhibit the Cdc25A and Cdc25B phosphatases (Fig. 1C). However, it was 50-fold less potent in inhibiting Cdc25C. The structural features of the catalytic domains of both Cdc25A and Cdc25B but not Cdc25C, have been solved [36,37]. Cdc25s, like the other PTPs and DSPs, contain the active site motif HCX5R. H is a highly conserved histidine, C is the catalytic cysteine, the X5 motif forms a loop with five amide nitrogen hydrogen bonds to the phosphate of the protein substrate, and R is a conserved arginine that binds to the phosphoamino acid of the substrate through two additional hydrogen bonds. Cdc25s have no sequence similarity with other PTPs outside the signature motif. The domain structures of Cdc25 outside the signature motif are also entirely different than the other PTPs and DSPs. The amino termini of Cdc25A, Cdc25B and Cdc25C share little homology and are thought likely to contribute to differences in the three isoforms. Therefore, it is probably not surprising to find a 50-fold difference in inhibition of Cdc25A or Cdc25B and Cdc25C by F-Cpd 5, or a more than 100-fold difference with MKP1 and PTP1B. However, inhibition profile of the Cdc25 isoenzymes by Cpd 5 was different than F-Cpd 5. Cpd 5 was found to inhibit all isoforms equally. This may suggest involvement of the fluoride atoms on F-Cpd 5 with the amino acids at the enzyme active site.

F-Cpd 5 was found to inhibit the growth of a spectrum of tumor cell lines with different potency, which ranged from 1 to 15 μM (Fig. 1B). Thus F-Cpd 5-induced growth inhibition was not specific only for Hep3B hepatoma cells. One other hepatoma cell line (PLC/PRF5) and tumor cells from breast, skin, stomach and colon were also inhibited.

An anti-cancer compound will have potential use only if it can inhibit tumor cells but spare normal surrounding cells. Since no normal hepatocyte derived cell lines are available, we tested primary rat hepatocytes for mitogen-induced DNA synthesis inhibition by F-Cpd 5. We found that normal rat hepatocytes were 12-fold less sensitive to growth inhibition by F-Cpd 5, when compared to the Hep3B hepatoma cells (Fig. 2). Thus F-Cpd 5 might be expected to have a useful therapeutic range. On comparison, mitogen-activated DNA synthesis of hepatocytes was only three-fold less sensitive to growth inhibition by Cpd 5 than Hep3B (Fig. 2). Thus difference in sensitivities of normal and tumor cells was greater for F-Cpd 5 than Cpd 5. Cpd 5 was found to inhibit liver tumors in rats without apparent toxicities [23] and both Cpd 5 and F-Cpd 5 inhibited hepatoma cells growth in vitro by similar mechanisms. Therefore, F-Cpd 5 is also predicted to be a potent tumor growth inhibitor in vivo without toxicities. Many anti-cancer compounds are known to have synergistic effect on tumors [44]. It will be interesting to test F-Cpd 5 together with doxorubicin or cisplatin, two commonly used drugs for hepatocellular carcinoma.

The role of Cdc25C-mediated dephosphorylation of Cdk1 at the G2/M transition has been clearly demonstrated [10]. The role of Cdc25A and Cdc25B in the dephosphorylation of Cdks during the cell cycle is less well defined. Cdc25A primarily acts on Cdk2 in G1/S transition, although its persistent activation during G2/M is consistent with it also acting on Cdk1. The main substrate of Cdc25B is postulated to be Cdk2 [8,9]. Although Cdc25C is the mitotic regulator at the G2/M transition, it has not been directly implicated in tumor development. Only Cdc25A and Cdc25B, but not Cdc25C, are over-expressed in human tumors [14–16]. It was interesting to find that F-Cpd 5 is 50-fold more potent in inhibiting Cdc25A and Cdc25B, than Cdc25C (Fig. 1C). It is therefore predicted to be effective against tumors which over-express Cdc25A or Cdc25B. We also found that the inhibitory tyrosine phosphorylation in Cdk2 and Cdk4 was induced in Hep3B cells treated with F-Cpd 5 (Fig. 3A). Moreover, dephosphorylation of tyrosine-phosphorylated Cdk4 by Hep3B cell lysate proteins were inhibited by F-Cpd 5 (Fig. 3B). These results were consistent with inhibition of Cdc25A and Cdc25B by F-Cpd 5 in Hep3B cells.

Our previous studies showed that PD 49, a biotin-tagged Cpd 5 derivative, bound to the catalytic cysteine of Cdc25B [22]. In PD 49, Br replaced the thioethanol side-chain of Cpd 5. Therefore, we synthesized a new Cpd 5-Bt derivative for this study, which now retained the thioethanol side-chain of Cpd 5. We assumed that both PD 49 and Cpd 5-Bt bind to the catalytic cysteine of Cdc25. Cpd 5-Bt was found to bind to both Cdc25A and Cdc25B. Increasing concentrations of F-Cpd 5 competed with this binding. We found a similar degree of competition between F-Cpd 5 and Cpd 5-Bt for binding to Cdc25A and Cdc25B (Fig. 4). This suggested that F-Cpd 5 most likely binds to the catalytic cysteine of Cdc25A and Cdc25B with similar binding efficiency. The binding of Cpd 5-Bt to Cdc25A or Cdc25B was not inhibited by an excess of MKP1 protein, another dual specificity phosphatase involved in cell signaling, suggesting that Cpd 5-Bt binds specifically to Cdc25A or Cdc25B.

F-Cpd 5-induced cell growth inhibition of the hepatoma cells Hep3B and PLC/PRF5 was found to be at least partly due to apoptosis. It was found to induce caspase-3 cleavage (Fig. 5A) and DNA laddering (Fig. 5B), two hallmarks of apoptosis, in response to F-Cpd 5.

Cpd 5-induced growth inhibition of Hep3B cells was found to be concomitant with a strong and prolonged phosphorylation of ERK1/2 [38,39]. Inhibition of this ERK phosphorylation also antagonized Cpd 5-induced growth inhibition [14] and, at least in some cells, was probably due to the inhibition of an ERK phosphatase and not due to the activation of an upstream kinase [40]. One of the candidate phosphatases of ERK was shown to be Cdc25A [35]. Thus the effect of Cpd 5 as a Cdc25A inhibitor was found to have a two-fold effect on the cells. It inhibited the activity of the Cdc25A substrates Cdk2 and Cdk4 to induce cell cycle arrest. Secondly, it induced strong ERK phosphorylation, which probably also induce cell death. F-Cpd 5 was also found to induce phosphorylation of the MAPKs JNK1/2 and p38 (Fig. 6) in addition to ERK, and inhibition by MAPK inhibitors antagonized F-Cpd 5-induced growth inhibition of Hep3B cells (Fig. 9). The data therefore support the hypothesis that F-Cpd 5 inhibited Hep3B cell growth by inhibiting Cdc25A and Cdc25B, which in turn caused cell cycle arrest as a result of inhibiting Cdk2 and Cdk4 actions and inducing MAPK phosphorylation. ERK is usually phosphorylated in response to a mitogenic signal. However, the cellular response to ERK phosphorylation is dependent on the net effects of the amplitude and duration of the activating signal [38,41]. We have shown that in response to Cpd 5 the transcription factor activities of Elk-1, Myc and CREB were inhibited [38,42,43]. However, in the presence of Cpd 5, persistent ERK phosphorylation occurs, and the same tran-

scription factor activities were inhibited [38,42]. Thus the phosphorylation of MAPKs by F-Cpd 5 are likely to be similarly involved in its mechanism(s) of inhibition of cell growth, since MAPK inhibitors antagonized its growth inhibitory effects.

The ability of F-Cpd 5 to inhibit ERK2 phosphatase(s) was supported by our finding that cell lysates contained ERK phosphatase activity, which was inhibited by F-Cpd 5 action (Fig. 7A). We showed that the ERK-selective phosphatase MKP1 was effective in pERK2 dephosphorylation but this activity was not inhibited by F-Cpd 5 (Fig. 7B). This suggested that the levels of MPK1 are negligible in Hep3B cells, and we confirmed this by our experiment (Fig. 8).

Fig. 1B shows the activity of F-Cpd 5 against several tumor cell lines from various organs. While the hepatocellular carcinoma line Hep3B was the most sensitive line, there was a spectrum of activity in the other lines. Growth inhibitory activity correlated with the induction of pERK (Fig. 8). The expression of MKP1 was negligible and expression of Cdc25A was high in the sensitive cells (Hep3B, PLC/PRL5, and FemX) compared to the resistant cells (SKBR3, LS140, and HR) (Fig. 8).

F-Cpd 5 thus represents a more potent analog of parent Cpd 5 and also represents an advance on its parent, by having a relatively selective effect on tumor cells compared with normal cells and generating less ROS. It also specifically inhibit Cdc25A and Cdc25B but much less of Cdc25C activities, likely by binding to their enzyme active site cysteines. It also induced MAPK phosphorylation and inhibited cell growth by inducing apoptosis.

Acknowledgment

This work was supported in part by the N.I.H. grant (CA 082723) to BIC.

REFERENCES

[1] Hunter T. Protein-kinases and phosphatases: the yin and yang of protein-phosphorylation and signaling. Cell 1995;80:225–36.
[2] Wera S, Hemmings BA. Serine/threonine protein phosphatases. Biochem J 1995;31:17–29.
[3] Keyse S. An energing family of dual specificity MAP-kinase phosphatases. Biochem Biophys Acta 1995;1265:152–60.
[4] Denu JM, Lohse DL, Vijayalakshmi J, Saper MA, Dixon JE. Visualization of intermediate and transition-state structures in protein-tyrosine-phosphatase catalysis. Proc Natl Acad Sci USA 1996;93:2493–8.
[5] Galaktionov K, Lee AK, Eckstein J, Draetta J, Meckler J, Loda M, et al. CDC25 phosphatases as potential human oncogenes. Science 1995;269:1575–7.
[6] Maehema T, Dixon JE. The tumor supressor, PTEN/MMAC1, dephosphorylates the lipid second messanger, phosphatidylinositol 3,4,5-triphosphate. J Biol Chem 1998;273:3375–13378.
[7] Nilsson I, Hoffman I. Cell cycle regulation by the Cdc25 phosphatase family. Prog Cell Cycle Res 2000;4:107–44.
[8] Jinno S, Suto J, Nagata A, Igarashi M, Kanaoka Y, Nojima H, et al. Cdc25A is a novel phosphatase functioning early in the cell cycle. EMBO J 1994;13:1549–56.
[9] Forrest AR, McCormack AK, DeSouza CP, Sinnamon JM, Tonks ID, Haywrd NK, et al. Multiple splicing variants of cdc25B regulate G2/M progression. Biochem Biophys Res Commun 1999;260:510–5.
[10] Donazelli M, Draetta GF. Regulating mammalian checkpoints through Cdc25 inactivation. EMBO J 2003;4:671–7.
[11] Molinari M, Mercurilo C, Dominguez J, Goubin F, Draetta GF. Human Cdca5A inactivation in response to S phase inhibition and its role in preventing premature mitosis. EMBO J 2000;1:71–9.
[12] Mailand N, Falck J, Lukas C, Syljuasen RG, Welcker M, Lukas J. Rapid destruction of human Cdc25A in response to DNA damage. Science 2000;288:1425–9.
[13] Parsons AR. Phosphatases and tumorigenesis. Curr Opin Oncol 1998;10:88–91.
[14] Kristjansdottir K, Rudolph J. Cdc25 phosphatases and cancer. Chem Biol 2004;11:1043–51.
[15] Gasparotto D, Maestro R, Piccinin S, Vukosavljevic T, Barzan L, Sulfaro S, et al. Overexpression of Cdc25A and Cdc25B in head and neck cancers. Cancer Res 1997;57:2366–3236.
[16] Hernandez S, Besser X, Bea S, et al. Differential expression of Cdc25 cell-cycle activating phosphatases in human colorectal carcinoma. Lab Invest 2001;81:465–70.
[17] Nishikawa Y, Carr BI, Wang Z, Kar S, Finn F, Dowd P, et al. Growth inhibition of hepatoma cells induced by Vitamin K and its analogs. J Biol Chem 1995;270:28304–10.
[18] Ni R, Nishikawa Y, Carr BI. Cell growth inhibition by a novel Vitamin K is associated with induction of protein tyrosine phosphorylation. J Biol Chem 1998;273:9906–11.
[19] Kerns J, Naganathan S, Dowd P, Finn F, Carr BI. Thioalkyl derivatives of Vitamin K3 and Vitamin K3 oxide inhibit growth of Hep 3B and Hep G2 cells. Bioorg Chem 1995;2:101–8.
[20] Lazo JS, Aslan DC, Southwick EC, Cooley KA, Ducruet AP, Joo B, et al. Discovery and biological evaluation of a new family of potent inhibitors of the dual specificity protein phosphatase Cdc25. J Med Chem 2001;44:4042–9.
[21] Lazo J, Nemoto K, Pestell KE, Cooley K, Southwick EC, Mitchell DA, et al. Identification of a potent and selective pharmacophore for Cdc25 dual specificity phosphatase inhibitors. Mol Pharmacol 2002;61:720–8.
[22] Kar S, Lefterov IM, Wang M, Lazo JS, Scott CN, Wilcox CS, et al. Binding and inhibition of Cdc25 phosphatases by Vitamin K analogues. Biochemistry 2003;42:10490–7.
[23] Kar S, Wang M, Ren Z, Chen X, Carr BI. Antitumor and anticarcinogenic action of Cpd 5: a new class of protein phosphatase inhibitor. Carcinogenesis 2003;24:411–6.
[24] Thor H, Smith MT, Hartzell P, Bellomo G, Jewell SA, Orrenius S. The metabolism of menadione (2-methyl-1,4-naphthoquinone) by isolated hepatocytes. A study of the implications of oxidative stress in intact cells. J Biol Chem 1982;257:12419–25.
[25] Morrison H, Jernstrom B, Nordenskjold M, Thor H, Orrenius S. Induction of DNA damage by menadione (2-methyl-1,4-naphthoquinone) in primary cultures of rat hepatocytes. Biochem Pharmacol 1984;33:1763–9.
[26] Han Y, Shen H, Carr BI, Wipf P, Lazo JS, Pan SS. NAD(P)H:quinone oxidoreductase-1-dependent and -independent cytotoxicity of potent quinone Cdc25 phosphatase inhibitors. J Pharmacol Exp Ther 2004; 309:64–70.
[27] Ham SW, Choe JI, Wang MF, Peyregne V, Carr BI. Fluorinated quinoid inhibitor: possible 'pure arylator' predicted by the simple theoretical calculation. Bioorg Med Chem Lett 2004;14:4103–5.
[28] Rago R, Mitchen J, Wilding G. DNA fluoremetric assay in 96-well tissue culture plates using Hoescht 33258 after cell lysis by freezing in distilled water. Anal Biochem 1990;191:31–4.

[29] Carr BI, Wang Z, Wang M, et al. A Cdc25A antagonizing K vitamin inhibits hepatocyte DNA synthesis in vitro and in vivo. J Mol Biol 2003;326:721–35.
[30] Bradford MM. A rapid and sensitive method for the quantitation of microgram quantities of protein utilizing the principle of protein–dye binding. Anal Biochem 1976;72:248–54.
[31] Kar S, Carr BI. Growth inhibition and protein tyrosine phosphorylation in MCF7 breast cancer cells by a novel K-vitamin. J Cell Physiol 2000;185:386–93.
[32] Tamura K, Southwick EC, Kerns J, Rosi K, Carr BI, Wilcox C, et al. Cdc25 inhibition and cell cycle arrest by a synthetic thioalkyl Vitamin K analogue. Cancer Res 2000;60:1317–25.
[33] Peyregne VP, Kar S, Ham SW, Wang M, Wang Z, Carr BI. Novel hydroxyl naphthoquinones with potent Cdc25 antagonizing and growth inhibitory properties. Mol Cancer Ther 2005;4:595–602.
[34] Maniatis T, Fritsch EF, Sambrook J. Molecular cloning New York: Cold Spring Harbor; 1982.
[35] Wang Z, Zhang B, Wang M, Carr BI. Cdc25A and ERK interaction: EGFR-independent ERK activation by a protein phosphatase Cdc25A inhibitor, compound 5. J Cell Physiol 2005;204:437–44.
[36] Fauman EB, Cogswell JP, Lovejoy B, Rocque WJ, Holmes W, Montana VG, et al. Crystal structure of the catalytic domain of the human cell cycle control phosphatase, Cdc25A. Cell 1998;93:617–25.
[37] Reynolds RA, Yem AW, Wolfe CL, Deibel Jr MR, Chidester CG, Watenpaugh KD. Crystal structure of the catalytic subunit of Cdc25B required for G2/M phase transition of the cell cycle. J Mol Biol 1999;293:559–68.
[38] Adachi T, Kar S, Wang M, Carr BI. Transient and sustained ERK phosphorylation and nuclear translocation in growth control. J Cell Physiol 2002;192:151–9.
[39] Osada S, Osada K, Carr BI. Tumor cell growth inhibition and extracellular signal-related kinase (ERK) phosphorylation by novel K vitamins. J Mol Biol 2001;314:765–72.
[40] Kar S, Adachi T, Carr BI. EGFR-independent activation of ERK1/2 mediates growth inhibition by a PTPase antagonizing K-vitamin analog. J Cell Physiol 2002;190: 356–64.
[41] Traverse S, Gomez N, Paterson H, Marshall C, Cohen P. Sustained activation of the mitogen-activated protein (MAP) kinase cascade may be required for differentiation of PC12 cells: comparison of the effects of nerve growth factor and epidermal growth factor. Biochem J 1992;288:351–5.
[42] Wang Z, Zhang B, Wang M, Carr BI. Persistent ERK phosphorylation negatively regulates cAMP response element-binding protein (CREB) activity via recruitment of CREB-binding protein to pp90RSK. J Biol Chem 2003;278:11138–44.
[43] Ge L, Wang Z, Wang M, Kar S, Carr BI. Involvement of c-Myc in growth inhibition of Hep3B human hepatoma cells by a Vitamin K analog. J Hepatol 2004;41:823–9.
[44] Park SH, Lee Y, Han SH, Kwon SW, et al. Systemic chemotherapy with doxorubicin, cisplatin and capecitabine for metastatic hepatocellular carcinoma. BMC Cancer 2006;6:1–6.